Chapter 4
Theory of Three-Dimensional Plasticity

Andreas Öchsner

Abstract This chapter presents a summary of the classical three-dimensional plasticity theory for rate-independent material behavior. The continuum modeling of plastic material behavior in relation to the constitutive equation comprises a yield condition, a flow rule, and a hardening rule. A special emphasis is given on the representation of yield conditions in the so-called invariant space. As typical examples in the context of classical plasticity theory, the conditions according to von Mises, Tresca, and Drucker-Prager are discussed in detail.

4.1 Comments on the Stress Matrix

Let us consider a three-dimensional body which is sufficiently supported and loaded (i.e., by any point or distributed loads) as schematically shown in Fig. 4.1a. Considering the symmetry of the stress matrix, six independent stress components, i.e., three normal and three shear stresses, can be identified, see Fig. 4.1b.

The stress components acting on a differential volume element may have, for example, the values as shown in Eq. (4.1) for the given (x, y, z) coordinate system. A coordinate transformation from the original (x, y, z) to the (x', y', z') coordinate system results in a stress matrix with different stress components, while a principal axis transformation (PAT) calculates the principal stresses σ_i, $(i = 1, 2, 3)$.

$$\sigma_{ij} = \begin{bmatrix} 50 & 0 & 20 \\ 0 & 80 & 20 \\ 20 & 20 & 90 \end{bmatrix}_{(x,y,z)} \overset{\text{rotation}}{\Rightarrow} \begin{bmatrix} 65 & 15 & 28.28 \\ 15 & 65 & 0 \\ 28.28427 & 0 & 90 \end{bmatrix}_{(x',y',z')} \overset{\text{PAT}}{\Rightarrow} \begin{bmatrix} 110 & 0 & 0 \\ 0 & 70 & 0 \\ 0 & 0 & 40 \end{bmatrix}_{(1,2,3)} . \tag{4.1}$$

A. Öchsner (✉)
Faculty of Mechanical and Systems Engineering, Esslingen University of Applied Sciences, Kanalstrasse 33, 73728 Esslingen, Germany
e-mail: andreas.oechsner@hs-esslingen.de

H. Altenbach et al. (eds.), *Lectures Notes on Advanced Structured Materials*,
Advanced Structured Materials 153, https://doi.org/10.1007/978-3-031-11589-9_4

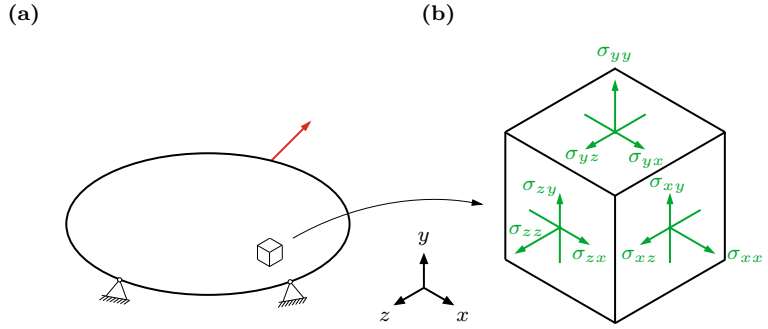

Fig. 4.1 **a** Three-dimensional body under arbitrary load and boundary conditions; **b** infinitesimal volume element with acting normal and shear stress components [see Altenbach and Öchsner (2020)]

Looking at this simple example, the following characteristics of the stress matrix can be summarized:

- The components of the stress matrix depend on the orientation of the user-defined coordinate system.
- There is a specific coordinate system (1, 2, 3) where the shear stresses vanish and only normal stresses remain on the main diagonal, i.e., the so-called principal stresses σ_i $(i = 1, 2, 3)$.
- The six or three stress components cannot easily be compared to experimental values from uniaxial tests (e.g., the initial yield stress in tension k_t^{init}).
- A graphical representation of any surface is much easier in a principal stress space (1, 2, 3) with three coordinates than in a space with six coordinates (σ_i).

Further information on continuum mechanics and plasticity theory can be taken from the classical textbooks by Backhaus (1983), Chen and Han (1988), Altenbach (2012), Altenbach et al. (1995), Betten (1987), Itskov (2009), and Itskov and Belyaev (2005). Let us review in the following the determination of the principal stresses and the axes directions of the corresponding (1, 2, 3) coordinate system. From a mathematical point of view, this question can be answered by determining the eigenvalues of the stress matrix (principal stresses) and the corresponding eigenvectors (principal directions). The solution of the so-called *characteristic equation*, i.e.,

$$\det\left(\sigma_{ij} - \sigma_i \mathrm{I}\right) = 0, \tag{4.2}$$

gives the three principal stresses σ_i $(i = 1, 2, 3)$. Equation (4.2) can be written in components as:

$$\det\left(\begin{bmatrix}\sigma_{xx} & \sigma_{xy} & \sigma_{xz}\\ \sigma_{yx} & \sigma_{yy} & \sigma_{yz}\\ \sigma_{zx} & \sigma_{zy} & \sigma_{zz}\end{bmatrix} - \sigma_i \begin{bmatrix}1 & 0 & 0\\ 0 & 1 & 0\\ 0 & 0 & 1\end{bmatrix}\right) = \det\left(\begin{bmatrix}\sigma_{xx}-\sigma_i & \sigma_{xy} & \sigma_{xz}\\ \sigma_{yx} & \sigma_{yy}-\sigma_i & \sigma_{yz}\\ \sigma_{zx} & \sigma_{zy} & \sigma_{zz}-\sigma_i\end{bmatrix}\right) = 0. \tag{4.3}$$

The calculation of the determinant ('det') results in the following cubic equation in σ_i:

$$\begin{aligned}&\sigma_i^3 - \underbrace{\left(\sigma_{xx}+\sigma_{yy}+\sigma_{zz}\right)}_{I_1}\sigma_i^2\\ &+ \underbrace{\left(\sigma_{xx}\sigma_{yy}+\sigma_{xx}\sigma_{zz}+\sigma_{yy}\sigma_{zz}-\sigma_{xy}^2-\sigma_{xz}^2-\sigma_{yz}^2\right)}_{I_2}\sigma_i\\ &- \underbrace{\left(\sigma_{xx}\sigma_{yy}\sigma_{zz}-\sigma_{xx}\sigma_{yz}^2-\sigma_{yy}\sigma_{xz}^2-\sigma_{zz}\sigma_{xy}^2+2\sigma_{xy}\sigma_{xz}\sigma_{yz}\right)}_{I_3} = 0,\end{aligned} \tag{4.4}$$

or in short:

$$\sigma_i^3 - I_1\sigma_i^2 + I_2\sigma_i - I_3 = 0, \tag{4.5}$$

where the three roots $(\sigma_1, \sigma_2, \sigma_3)$ of Eq. (4.5) are the principal stresses. Equation (4.4) can be used to define the three scalar so-called principal invariants I_1, I_2, and I_3. These tensor invariants are independent of the orientation of the coordinate system (objectivity) and represent the physical content of the stress matrix.

The coordinates of the ith eigenvector (x_i, y_i, z_i)—which correspond to the direction of one of the new $(1, 2, 3)$ coordinate axes—result from the following system of three equations:

$$\begin{bmatrix}\sigma_{xx}-\sigma_i & \sigma_{xy} & \sigma_{xz}\\ \sigma_{yx} & \sigma_{yy}-\sigma_i & \sigma_{yz}\\ \sigma_{zx} & \sigma_{zy} & \sigma_{zz}-\sigma_i\end{bmatrix}\begin{bmatrix}x_i\\ y_i\\ z_i\end{bmatrix} = \begin{bmatrix}0\\ 0\\ 0\end{bmatrix}. \tag{4.6}$$

Let us mention at this point that the determination of the eingenvalues and eigenvectors is also common in applied mechanics for other tensors or matrices. The second moment of the area tensor (or the moment of inertia tensor) has similar properties as the stress matrix:

$$\begin{bmatrix}I_{xx} & I_{xy} & I_{xz}\\ I_{yx} & I_{yy} & I_{yz}\\ I_{zx} & I_{zy} & I_{zz}\end{bmatrix}_{(x,y,z)} \overset{\text{PAT}}{\Rightarrow} \begin{bmatrix}I_1 & 0 & 0\\ 0 & I_2 & 0\\ 0 & 0 & I_3\end{bmatrix}_{(1,2,3)}. \tag{4.7}$$

Let us look in the following a bit closer at the stress invariants[1]. Another interpretation of the *principal* stress invariants is given by Chen and Han (1988):

[1] It is useful for some applications (e.g., the calculation of the derivative with respect to the stresses) to *not* consider the symmetry of the shear stress components and to work with nine stress components. These invariants are denoted by $\underline{I}_i$ and $\underline{J}_i$.

Table 4.1 Definition of the three principal (I_i) and basic (J_i) stress invariants of the stress matrix

First stress invariant of σ_{ij}
$I_1 = \sigma_{xx} + \sigma_{yy} + \sigma_{zz}$
$J_1 = \sigma_{xx} + \sigma_{yy} + \sigma_{zz}$
Second stress invariant of σ_{ij}
$I_2 = \sigma_{xx}\sigma_{yy} + \sigma_{xx}\sigma_{zz} + \sigma_{yy}\sigma_{zz} - \sigma_{xy}^2 - \sigma_{xz}^2 - \sigma_{yz}^2$
$J_2 = \frac{1}{2}\left(\sigma_{xx}^2 + \sigma_{yy}^2 + \sigma_{zz}^2\right) + \sigma_{xy}^2 + \sigma_{xz}^2 + \sigma_{yz}^2$
Third stress invariant of σ_{ij}
$I_3 = \sigma_{xx}\sigma_{yy}\sigma_{zz} - \sigma_{xx}\sigma_{yz}^2 - \sigma_{yy}\sigma_{xz}^2 - \sigma_{zz}\sigma_{xy}^2 + 2\sigma_{xy}\sigma_{xz}\sigma_{yz}$
$J_3 = \frac{1}{3}\left(\sigma_{xx}^3 + \sigma_{yy}^3 + \sigma_{zz}^3 + 3\sigma_{xy}^2\sigma_{xx} + 3\sigma_{xy}^2\sigma_{yy} + 3\sigma_{xz}^2\sigma_{xx} + 3\sigma_{xz}^2\sigma_{zz}\right.$
$\left.+3\sigma_{yz}^2\sigma_{yy} + 3\sigma_{yz}^2\sigma_{zz} + 6\sigma_{xy}\sigma_{xz}\sigma_{yz}\right)$

– I_1 = sum of the diagonal terms of σ_{ij}:

$$I_1 = \sigma_{xx} + \sigma_{yy} + \sigma_{zz}. \tag{4.8}$$

– I_2 = sum of the two-row main subdeterminants:

$$I_2 = \begin{vmatrix} \sigma_{xx} & \sigma_{xy} \\ \sigma_{xy} & \sigma_{yy} \end{vmatrix} + \begin{vmatrix} \sigma_{yy} & \sigma_{yz} \\ \sigma_{yz} & \sigma_{zz} \end{vmatrix} + \begin{vmatrix} \sigma_{xx} & \sigma_{xz} \\ \sigma_{xz} & \sigma_{zz} \end{vmatrix}. \tag{4.9}$$

– I_3 = determinant of σ_{ij}:

$$I_3 = \begin{vmatrix} \sigma_{xx} & \sigma_{xy} & \sigma_{xz} \\ \sigma_{xy} & \sigma_{yy} & \sigma_{yz} \\ \sigma_{xz} & \sigma_{yz} & \sigma_{zz} \end{vmatrix}. \tag{4.10}$$

Besides these principal invariants, there is also often another set of invariants used. This set is included in the principal invariants and called *basic invariants* [see Backhaus (1983)]:

$$J_1 = I_1, \tag{4.11}$$

$$J_2 = \frac{1}{2}I_1^2 - I_2, \tag{4.12}$$

$$J_3 = \frac{1}{3}I_1^3 - I_1 I_2 + I_3. \tag{4.13}$$

The definition of both sets of invariants is given in Table 4.1.

It is common in the framework of the plasticity theory of isotropic materials to decompose the stress matrix σ_{ij} into a pure volume changing (spherical or hydrostatic) matrix σ_{ij}^{o} and a pure shape changing (deviatoric) stress matrix s_{ij} (cf. Fig. 4.2)[2]:

[2] It should be noted that in the case of anisotropic materials, a hydrostatic stress state may result in a shape change (Betten 2001).

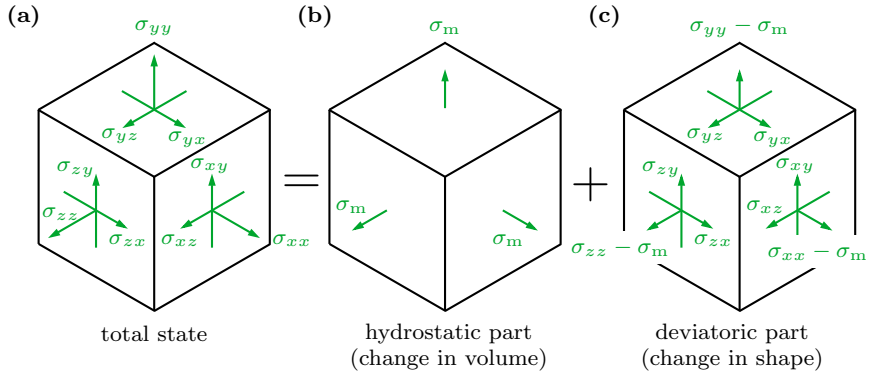

Fig. 4.2 Decomposition of the stress matrix **a** into its spherical **b** and the deviatoric **c** part

$$\sigma_{ij} = \sigma_{ij}^{\mathrm{o}} + s_{ij} = \sigma_{\mathrm{m}}\mathbf{I} + s_{ij}. \tag{4.14}$$

In Eq. (4.14), $\sigma_{\mathrm{m}} = \frac{1}{3}(\sigma_{xx} + \sigma_{yy} + \sigma_{zz})$ denotes the mean normal stress[3] and $\mathbf{I}$ the identity matrix. Furthermore, Einstein's summation convention was used [see Moore (2013)].

Equation (4.14) can be written in components as

$$\underbrace{\begin{bmatrix} \sigma_{xx} & \sigma_{xy} & \sigma_{xz} \\ \sigma_{xy} & \sigma_{yy} & \sigma_{yz} \\ \sigma_{xz} & \sigma_{yz} & \sigma_{zz} \end{bmatrix}}_{\text{stress matrix } \sigma_{ij}} = \underbrace{\begin{bmatrix} \sigma_{\mathrm{m}} & 0 & 0 \\ 0 & \sigma_{\mathrm{m}} & 0 \\ 0 & 0 & \sigma_{\mathrm{m}} \end{bmatrix}}_{\text{hydrostatic matrix } \sigma_{ij}^{\mathrm{o}}} + \underbrace{\begin{bmatrix} s_{xx} & s_{xy} & s_{xz} \\ s_{xy} & s_{yy} & s_{yz} \\ s_{xz} & s_{yz} & s_{zz} \end{bmatrix}}_{\text{deviatoric matrix } s_{ij}}. \tag{4.15}$$

It can be seen that the elements outside the diagonal terms, i.e., the shear stresses, are the same for the stress and the deviatoric stress matrix

$$s_{ij} = \sigma_{ij} \quad \text{for} \quad i \neq j, \tag{4.16}$$

$$s_{ij} = \sigma_{ij} - \sigma_{\mathrm{m}} \quad \text{for} \quad i = j, \tag{4.17}$$

and it can be shown that the so-called deviator equation

$$s_{xx} + s_{yy} + s_{zz} = 0 \tag{4.18}$$

holds. The following list summarizes the calculation of the stress deviator components:

[3] Also called the hydrostatic stress; in the context of soil mechanics, the pressure $p = -\sigma_{\mathrm{m}}$ is also used.

Table 4.2 Definition of the three principal (I_i°) and basic (J_i°) stress invariants of the hydrostatic stress matrix σ_{ij}°

First stress invariant of σ_{ij}°
$I_1^\circ = 3\sigma_\mathrm{m}$
$J_1^\circ = 3\sigma_\mathrm{m}$
Second stress invariant of σ_{ij}°
$I_2^\circ = 3\sigma_\mathrm{m}^2$
$J_2^\circ = \frac{3}{2}\sigma_\mathrm{m}^2$
Third stress invariant of σ_{ij}°
$I_3^\circ = \sigma_\mathrm{m}^3$
$J_3^\circ = \sigma_\mathrm{m}^3$

Table 4.3 Definition of the three principal (I_i') and basic (J_i') stress invariants of the deviatoric stress matrix s_{ij}

First stress invariant of s_{ij}
$I_1' = 0$
$J_1' = 0$
Second stress invariant of s_{ij}
$I_2' = s_{xx}s_{yy} + s_{xx}s_{zz} + s_{yy}s_{zz} - s_{xy}^2 - s_{xz}^2 - s_{yz}^2$
$J_2' = -I_2'$
Third stress invariant of s_{ij}
$I_3' = s_{xx}s_{yy}s_{zz} - s_{xx}s_{yz}^2 - s_{yy}s_{xz}^2 - s_{zz}s_{xy}^2 + 2s_{xy}s_{xz}s_{yz}$
$J_3' = I_3'$

$$s_{xx} = \sigma_{xx} - \sigma_\mathrm{m} = \frac{2}{3}\sigma_{xx} - \frac{1}{3}(\sigma_{yy} + \sigma_{zz}), \tag{4.19}$$

$$s_{yy} = \sigma_{yy} - \sigma_\mathrm{m} = \frac{2}{3}\sigma_{yy} - \frac{1}{3}(\sigma_{xx} + \sigma_{zz}), \tag{4.20}$$

$$s_{zz} = \sigma_{zz} - \sigma_\mathrm{m} = \frac{2}{3}\sigma_{zz} - \frac{1}{3}(\sigma_{xx} + \sigma_{yy}), \tag{4.21}$$

$$s_{xy} = \sigma_{xy}, \tag{4.22}$$

$$s_{yz} = \sigma_{yz}, \tag{4.23}$$

$$s_{xz} = \sigma_{xz}. \tag{4.24}$$

The definitions of the principal and basic invariants can be applied directly to the hydrostatic and deviatoric part of the stress matrix to obtain a similar representation as provided in Table 4.1, see summary in Table 4.2 for the hydrostatic matrix and the summary in Table 4.3 for the deviatoric matrix.

The hydrostatic part of σ_{ij} has in the case of metallic materials (full dense materials) for temperatures approximately under 0.3 T_{mt} (T_{mt}: melting temperature) nearly no influence on the occurrence of inelastic strains since dislocations slip only under the influence of shear stresses (for higher temperatures from 0.3 till 0.5 T_{m} also non-conservative climbing is possible) (Suzuki et al. 1985). On the other hand, the hydrostatic stress has a considerable influence on the yielding behavior in the case of soil mechanics, cellular materials or in damage mechanics (formation of pores, e.g., Gurson (1977)).

The evaluation of the basic invariants for the stress matrix, as well as the hydrostatic and deviatoric part is presented in Table 4.4, expressed in components of σ_{ij} and the principal stresses $\sigma_1, \sigma_2, \sigma_3$.

It can be seen in Table 4.4 that the spherical matrix is completely characterized by its first invariant because the second and third invariant are powers of it. The stress deviator matrix is completely characterized by its second and third invariant. Therefore, the physical contents of the stress state σ_{ij} can be described either by the

Table 4.4 Basic invariants in terms of σ_{ij} and principal values

Invariants	Components of σ_{ij}	Principal stresses $\sigma_1, \sigma_2, \sigma_3$
Stress matrix		
J_1	$\sigma_{xx} + \sigma_{yy} + \sigma_{zz}$	$\sigma_1 + \sigma_2 + \sigma_3$
J_2	$\frac{1}{2}\left(\sigma_{xx}^2 + \sigma_{yy}^2 + \sigma_{zz}^2\right) + \sigma_{xy}^2 + \sigma_{xz}^2 + \sigma_{yz}^2$	$\frac{1}{2}\left(\sigma_1^2 + \sigma_2^2 + \sigma_3^2\right)$
J_3	$\frac{1}{3}\left(\sigma_{xx}^3 + \sigma_{yy}^3 + \sigma_{zz}^3 + 3\sigma_{xy}^2\sigma_{xx} + 3\sigma_{xy}^2\sigma_{yy} + 3\sigma_{xz}^2\sigma_{xx} + 3\sigma_{xz}^2\sigma_{zz} + 3\sigma_{yz}^2\sigma_{yy} + 3\sigma_{yz}^2\sigma_{zz} + 6\sigma_{xy}\sigma_{xz}\sigma_{yz}\right)$	$\frac{1}{3}\left(\sigma_1^3 + \sigma_2^3 + \sigma_3^3\right)$
Spherical matrix		
J_1^{o}	$\sigma_{xx} + \sigma_{yy} + \sigma_{zz}$	$\sigma_1 + \sigma_2 + \sigma_3$
J_2^{o}	$\frac{1}{6}\left(\sigma_{xx} + \sigma_{yy} + \sigma_{zz}\right)^2$	$\frac{1}{6}\left(\sigma_1 + \sigma_2 + \sigma_3\right)^2$
J_3^{o}	$\frac{1}{27}\left(\sigma_{xx} + \sigma_{yy} + \sigma_{zz}\right)^3$	$\frac{1}{27}\left(\sigma_1 + \sigma_2 + \sigma_3\right)^3$
Stress deviator matrix		
J_1'	0	0
J_2'	$\frac{1}{6}\left[(\sigma_{xx} - \sigma_{yy})^2 + (\sigma_{yy} - \sigma_{zz})^2 + (\sigma_{zz} - \sigma_{xx})^2\right] + \sigma_{xy}^2 + \sigma_{yz}^2 + \sigma_{zx}^2$	$\frac{1}{6}\left[(\sigma_1 - \sigma_2)^2 + (\sigma_2 - \sigma_3)^2 + (\sigma_3 - \sigma_1)^2\right]$
J_3'	$s_{xx}s_{yy}s_{zz} + 2\sigma_{xy}\sigma_{yz}\sigma_{zx} - s_{xx}\sigma_{yz}^2 - s_{yy}\sigma_{zx}^2 - s_{zz}\sigma_{xy}^2$	$s_1 s_2 s_3$
With	$s_{xx} = \frac{1}{3}(2\sigma_{xx} - \sigma_{yy} - \sigma_{zz})$	$s_1 = \frac{1}{3}(2\sigma_1 - \sigma_2 - \sigma_3)$
	$s_{yy} = \frac{1}{3}(-\sigma_{xx} + 2\sigma_{yy} - \sigma_{zz})$	$s_2 = \frac{1}{3}(-\sigma_1 + 2\sigma_2 - \sigma_3)$
	$s_{zz} = \frac{1}{3}(-\sigma_{xx} - \sigma_{yy} + 2\sigma_{zz})$	$s_3 = \frac{1}{3}(-\sigma_1 - \sigma_2 + 2\sigma_3)$
	$s_{xy} = \sigma_{xy}, s_{xz} = \sigma_{xz}, s_{yz} = \sigma_{yz}$	

Table 4.5 Basic invariants for the $\sigma_1 - \sigma_2$ and $\sigma - \tau$ space

Invariants	$\sigma_1 - \sigma_2$ space	$\sigma - \tau$ space
J_1^{o}	$\sigma_1 + \sigma_2$	σ
J_2'	$\frac{1}{3}\left(\sigma_1^2 + \sigma_2^2 - \sigma_1\sigma_2\right)$	$\frac{1}{3}\sigma^2 + \tau^2$
J_3'	$\frac{1}{27}\left(2\sigma_1^3 + 2\sigma_2^3 - 3\sigma_1\sigma_2(\sigma_1 + \sigma_2)\right)$	$\frac{2}{27}\sigma^3 + \frac{1}{3}\sigma\tau^2$

Table 4.6 Basic invariants for a uniaxial (normal) stress (σ) state and a pure shear stress state (τ)

Invariants	Only σ	Only τ
J_1^{o}	σ	0
J_2'	$\frac{1}{3}\sigma^2$	τ^2
J_3'	$\frac{2}{27}\sigma^3$	0

three basic stress invariants J_i or if we use the decomposition in its spherical and deviatoric part by the first invariant of the spherical matrix and the second and third invariant of the stress deviator matrix. In the following, we will only use these three basic invariants to describe yield and failure conditions. Thus, the physical content of a state of stress will be described by the following set of invariants:

$$\sigma_{ij} \;\rightarrow\; J_1^{\mathrm{o}},\, J_2',\, J_3'. \tag{4.25}$$

To derive important special cases of yield conditions, it is also useful to specify the stress invariants for a plane stress state $\sigma_1 - \sigma_2$ and a stress state $\sigma - \tau$ where only one normal and one shear stress is acting. Thus, the stress invariants reduce to the given form in Table 4.5.

Finally, Table 4.6 summarizes the stress invariants for a uniaxial or pure shear stress state.

The representation of a tress state in terms of invariants is also very useful in the context of the implementation of yield conditions into commercial finite elements codes. This significantly facilities the calculation of derivatives [see Öchsner (2003)].

4.2 Graphical Representation of Yield Conditions

Plastic flow starts in a uniaxial tensile test as soon as the acting tensile stress σ reaches the initial yield stress k^{init}, see Öchsner (2016). In the case of a multiaxial stress state, this simple comparison is replaced by the yield condition. To this end, a scalar value is calculated from the acting six stress components and compared to an experimental scalar value. The yield condition in stress space can be expressed in its most general form ($\mathrm{IR}^6 \times \mathrm{IR}^{\dim(q)} \rightarrow \mathrm{IR}$) as:

$$F = F(\boldsymbol{\sigma}, \boldsymbol{q}). \tag{4.26}$$

For further characterization, we assume in the following the special case of ideal plastic material behavior (vector of hardening variables $\boldsymbol{q} = \mathbf{0}$) so that for ($\mathrm{IR}^6 \rightarrow \mathrm{IR}$)

$$F = F(\boldsymbol{\sigma}) \tag{4.27}$$

depends now only on the stress state. The values of F have—as in the uniaxial case—the following[4] mechanical meaning:

$$F(\boldsymbol{\sigma}) = 0 \rightarrow \text{plastic material behavior}, \tag{4.28}$$

$$F(\boldsymbol{\sigma}) < 0 \rightarrow \text{elastic material behavior}, \tag{4.29}$$

$$F(\boldsymbol{\sigma}) > 0 \rightarrow \text{invalid}. \tag{4.30}$$

A further simplification is obtained under the assumption that the yield condition can be split in a pure stress part $f(\boldsymbol{\sigma})$ and an experimental material parameter k:

$$F(\boldsymbol{\sigma}) = f(\boldsymbol{\sigma}) - k. \tag{4.31}$$

The yield condition $F = 0$ represents in a n-dimensional space a hypersurface that is also called the yield surface or the yield loci. The number n is equal to the independent stress matrix components. A direct graphical representation of the yield surface is not possible due to its dimensionality, i.e., six variables. However, a reduction of the dimensionality is possible to achieve if a principle axis transformation [see Eq. (4.2)] is applied to the argument σ_{ij}. The components of the stress matrix reduce to the principal stresses σ_1, σ_2, and σ_3 on the principal diagonal of the stress matrix and the non-diagonal elements are equal to zero. In such a principal stress space, it is possible to graphically represent the yield condition as a three-dimensional surface. This space is also called the Haigh-Westergaard stress space [see Chen and Zhang (1991)]. A hydrostatic stress state lies in such a principal stress system on the space diagonal (hydrostatic axis). Any plane perpendicular to the hydrostatic axis is called an octahedral plane. The particular octahedral plane passing through the origin is called the deviatoric plane or π-plane [see Chen and Han (1988)]. Because $\sigma_1 + \sigma_2 + \sigma_3 = 0$, it follows from Eq. (4.14) that $\sigma_{ij} = s_{ij}$, i.e., any stress state on the π-plane is pure deviatoric.

The possibility of a representation of a yield condition based on a set of independent stress invariants (e.g., according to Eq. (4.25)) is the characteristic of any isotropic yield condition, regardless of the choice of coordinate system. Therefore, Eq. (4.27) can also be written as

$$F = F(J_1^{\mathrm{o}}, J_2', J_3'). \tag{4.32}$$

[4] Under the restriction of rate-independent plasticity.

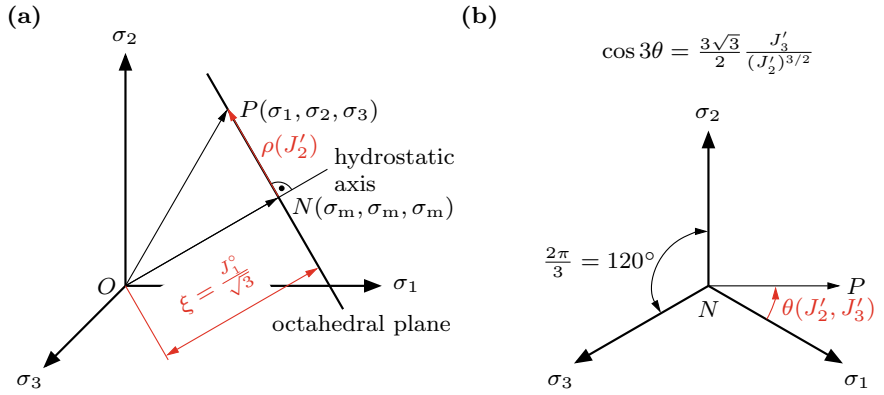

Fig. 4.3 Geometrical interpretation of basic stress invariants: **a** principal stress space; **b** octahedral plane

On the basis of the dependency of the yield condition on the invariants, a descriptive classification can be performed. Yield conditions independent of the hydrostatic stress (J_1^o) can be represented by the invariants J_2' and J_3'. Stress states with $J_2' = \text{const.}$ lie on a circle around the hydrostatic axis in an octahedral plane. A dependency of the yield condition on J_3' results in a deviation from the circle shape. The yield surface forms a prismatic body whose longitudinal axis is represented by the hydrostatic axis. A dependency on J_1^o denotes a size change of the cross section of the yield surface along the hydrostatic axis. However, the shape of the cross section remains similar in the mathematical sense. Therefore, a dependency on J_1^o can be represented by sectional views through planes along the hydrostatic axis.

The geometrical interpretation of stress invariants [see Chen and Han (1988)] is given in Fig. 4.3.

It can be seen that an arbitrary stress state P can be expressed by its position along the hydrostatic axis $\xi = \frac{1}{\sqrt{3}} J_1^o$ and its polar coordinates ($\rho = \sqrt{2J_2'}, \theta(J_2', J_3')$) in the octahedral plane through P. For the set of polar coordinates, the so-called stress Lode angle θ is defined in the range $0 \leq \theta \leq 60°$ as [see Nayak and Zienkiewicz (1972)],

$$\cos(3\theta) = \frac{3\sqrt{3}}{2} \cdot \frac{J_3'}{(J_2')^{3/2}}. \tag{4.33}$$

It can be concluded from Eq. (4.33) that

$$3\theta = 3\theta(J_2', J_3'), \tag{4.34}$$

or that

$$\theta = \theta(J_2', J_3'). \tag{4.35}$$

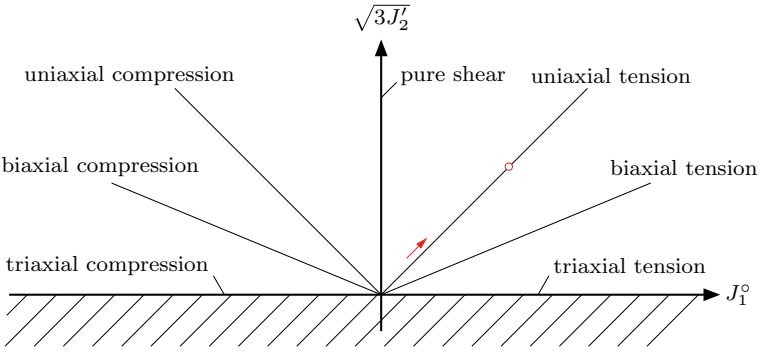

Fig. 4.4 Schematic representation of basic tests in the J_1°-$\sqrt{3J_2'}$ invariant space

Fig. 4.5 Identification of the shape of a yield condition in an octahedral plane ($\sigma_\mathrm{m} = \text{const.}$)

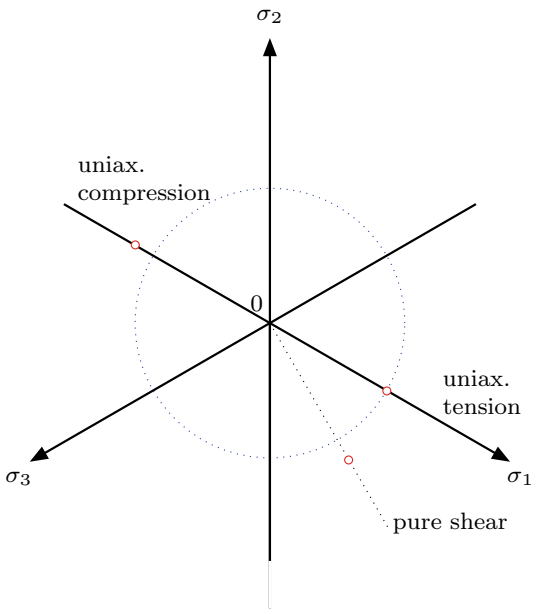

The trigonometric identity $\cos(3\theta) = 4\cos^3(\theta) - 3\cos(\theta)$ may be used for some transformations.

The set of coordinates $(\xi, \rho, \cos(3\theta))$ is known in the literature as the Haigh-Westergaard coordinates. To investigate the shape of the yield surface, particular experiments, including multiaxial stress states, must be realized and the initial yield points marked and approximated in the Haigh-Westergaard space, the J_1°-$\sqrt{3J_2'}$ invariant space, and octahedral planes, see Figs. 4.4 and 4.5.

Table 4.7 Definition of basic tests in the J_1°-$\sqrt{3J_2'}$ invariant space

Case	J_1°	$\sqrt{3J_2'}$	Comment
Uniax. tension (σ)	σ	σ	Slope: 1
Uniax. compression ($-\sigma$)	$-\sigma$	σ	Slope: -1
Biax. tension (σ)	2σ	σ	Slope: 0.5
Biax. compression ($-\sigma$)	-2σ	σ	Slope: -0.5
Triax. tension (σ)	3σ	0	Horiz. axis
Triax. compression ($-\sigma$)	-3σ	0	Horiz. axis
Pure shear (τ)	0	$\sqrt{3}\,\tau$	Vertical axis

The loading path, for example, for the biaxial tension case in the J_1°-$\sqrt{3J_2'}$ invariant space (see Fig. 4.4) is obtained as follows (see Table 4.5 for the evaluation of the invariants):

$$\sqrt{3J_2'} = \sigma = \frac{1}{2} J_1^{\circ} \tag{4.36}$$

Further load paths for basic experiments in the $J_1^{\circ} - \sqrt{3J_2'}$ invariant space are summarized in Table 4.7.

4.3 Yield Conditions

The yield condition can generally be expressed as

$$F(\boldsymbol{\sigma}, \boldsymbol{q}) \leq 0, \tag{4.37}$$

where $\boldsymbol{q} = \left[\kappa \ \boldsymbol{\alpha}\right]^{\mathrm{T}}$ is the column matrix of internal variables describing the hardening behavior of the material. Parameter κ relates to isotropic hardening, while the matrix $\boldsymbol{\alpha}$ contains the kinematic hardening parameters. The mechanical meaning of F remains as indicated by Eqs. (4.28)–(4.30).

Restricting to isotropic hardening, Eq. (4.37) can be expressed as

$$F(\boldsymbol{\sigma}, \kappa) \leq 0. \tag{4.38}$$

4.3.1 Mises Yield Condition

The total deformation energy per unit volume of a three-dimensional body can be generally expressed as [see Öchsner (2016)]:

$$w = \frac{1}{2}\left(\sigma_{xx}\varepsilon_{xx} + \sigma_{yy}\varepsilon_{yy} + \sigma_{zz}\varepsilon_{zz} + \tau_{xy}\gamma_{xy} + \tau_{xz}\gamma_{xz} + \tau_{yz}\gamma_{yz}\right). \tag{4.39}$$

Following the decomposition of the stress matrix in its spherical and deviatoric part as indicated in Fig. 4.2, this deformation energy can be split in its volumetric (w°) and distortional (w^{s}) part as:

$$w = \underbrace{\frac{1-2\nu}{6E}\left(\sigma_{xx} + \sigma_{yy} + \sigma_{zz}\right)^2}_{w^{\circ}} + \\ + \underbrace{\frac{1+\nu}{6E}\left[(\sigma_{xx} - \sigma_{yy})^2 + (\sigma_{yy} - \sigma_{zz})^2 + (\sigma_{zz} - \sigma_{xx})^2 + 6(\tau_{xy}^2 + \tau_{yz}^2 + \tau_{xz}^2)\right]}_{w^{s}}. \tag{4.40}$$

The von Mises yield condition states now that plastic deformation starts as soon as the distortional deformation energy per unit volume, i.e.,

$$w^{s} = \frac{1+\nu}{6E}\left[(\sigma_{xx} - \sigma_{yy})^2 + (\sigma_{yy} - \sigma_{zz})^2 + (\sigma_{zz} - \sigma_{xx})^2 + 6(\tau_{xy}^2 + \tau_{yz}^2 + \tau_{xz}^2)\right], \tag{4.41}$$

reaches a critical value ($k_t^2/(6G)$) [see Asaro and Lubarda (2006), Nash (1998)]. This yield condition is commonly applied for ductile metals. The expression in units of stress is given for a general three-dimensional stress state as

$$F(\sigma_{ij}) = \\ \underbrace{\sqrt{\frac{1}{2}\left((\sigma_x - \sigma_y)^2 + (\sigma_y - \sigma_z)^2 + (\sigma_z - \sigma_x)^2\right) + 3\left(\sigma_{xy}^2 + \sigma_{yz}^2 + \sigma_{xz}^2\right)}}_{\sigma_{\text{eff}}} - k_t = 0, \tag{4.42}$$

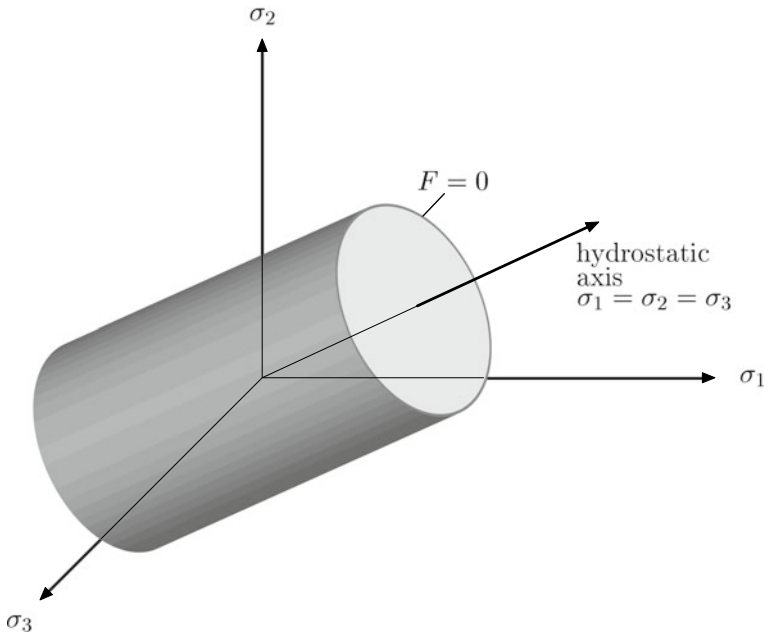

Fig. 4.6 Graphical representation of the yield condition according to von Mises in the principal stress space

or in the principal stress space $(\sigma_1, \sigma_2, \sigma_3)$ with $\sigma_{xy} = \sigma_{yz} = \sigma_{xz} = 0$:

$$F(\sigma_{ij}) = \underbrace{\sqrt{\frac{1}{2}\left((\sigma_1 - \sigma_2)^2 + (\sigma_2 - \sigma_3)^2 + (\sigma_3 - \sigma_1)^2\right)}}_{\sigma_{\text{eff}}} - k_{\text{t}} = 0. \tag{4.43}$$

The graphical representation in the principal stress space is given in Fig. 4.6, where a cylinder with its longitudinal axis equal to the hydrostatic axis is obtained.

Expressed with the second invariant of the stress deviator (see Table 4.4), one can write the following formulation:

$$F(J_2') = \sqrt{3J_2'} - k_{\text{t}} = 0. \tag{4.44}$$

The representation in the $\sqrt{3J_2'}$-J_1° space (see Fig. 4.8) shows that the yield condition is independent of the hydrostatic stress (Fig. 4.7).

The view along the hydrostatic axis is shown in Fig. 4.8 where it can be seen that there is no difference under tension and compression for uniaxial stress states.

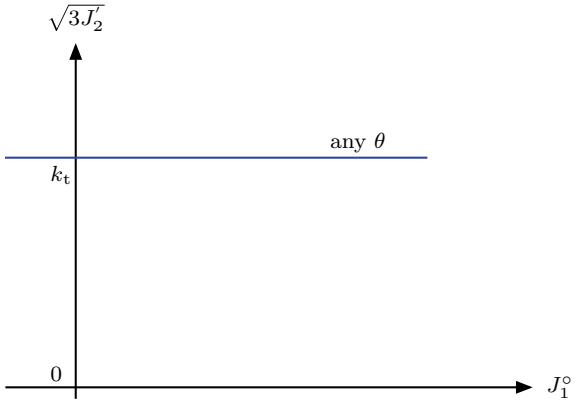

Fig. 4.7 Graphical representation of the yield condition according to von Mises in the $\sqrt{3J_2'}$-J_1° space

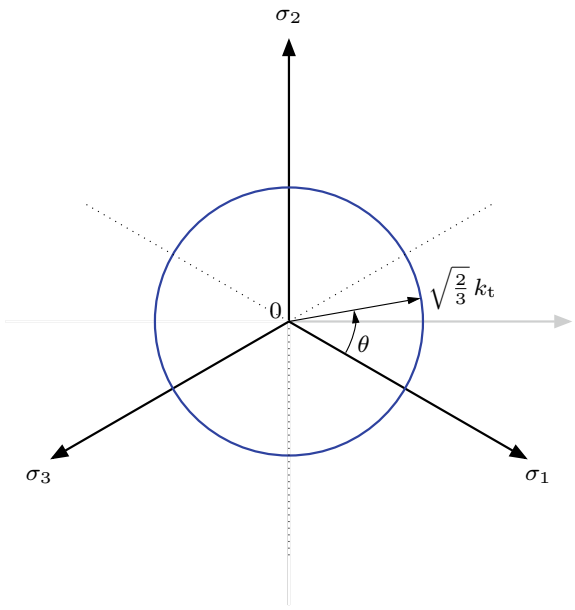

Fig. 4.8 Graphical representation of the yield condition according to von Mises in the octahedral plane

A representation in the two-component principal σ_1–σ_2 space is obtained by substituting the particular basic invariant formulations from Table 4.5 into Eq. (4.44) as (see Fig. 4.9):

$$F_{\sigma_1-\sigma_2} = \sigma_1^2 + \sigma_2^2 - \sigma_1\sigma_2 - k_t^2 = 0, \tag{4.45}$$

or represented in a standard form to easier identify an ellipse (see Fig. 4.9) as

$$F_{\sigma_1-\sigma_2} = \left(\frac{x}{\sqrt{2}\,k_t}\right)^2 + \left(\frac{y}{\sqrt{2}\,k_s}\right)^2 - 1 = 0, \tag{4.46}$$

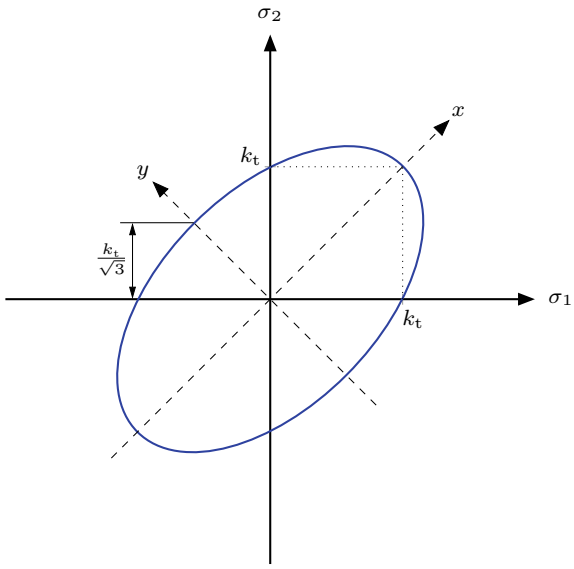

Fig. 4.9 Graphical representation of the yield condition according to von Mises in the σ_1-σ_2 space

where $x = (\sigma_1 + \sigma_2)/\sqrt{2}$ and $y = (\sigma_2 - \sigma_1)/\sqrt{2}$.

The transformation of Eq. (4.45) into Eq. (4.46) can be obtained in the following way:

$$\sigma_1^2 + \sigma_2^2 - \sigma_1\sigma_2 = k_t^2, \tag{4.47}$$

$$4\sigma_1^2 + 4\sigma_2^2 - 4\sigma_1\sigma_2 = 4k_t^2, \tag{4.48}$$

$$\sigma_1^2 + 2\sigma_1\sigma_2 + \sigma_2^2 + 3(\sigma_1^2 - 2\sigma_1\sigma_2 + \sigma_2^2) = 4k_t^2, \tag{4.49}$$

$$\frac{1}{4}(\sigma_1 + \sigma_2)^2 + \frac{3}{4}(\sigma_2 - \sigma_1)^2 = k_t^2, \tag{4.50}$$

$$\left(\frac{\sigma_1 + \sigma_2}{2\,k_t}\right)^2 + \left(\frac{\sigma_2 - \sigma_1}{2\,\frac{k_s}{\sqrt{3}}}\right)^2 = 1. \tag{4.51}$$

A representation in the two-component normal/shear σ-τ space is obtained by substituting the particular basic invariant formulations from Table 4.5 into Eq. (4.44) to finally give the following ellipse (see Fig. 4.10):

$$F_{\sigma-\tau} = \left(\frac{\sigma}{k_t}\right)^2 + \left(\frac{\sqrt{3}\,\tau}{k_t}\right)^2 - 1 = 0. \tag{4.52}$$

The last formulation allows to identify the relationship between the shear and tensile yield stress. Setting $\sigma = 0$, which means then $\tau \to k_s$, gives:

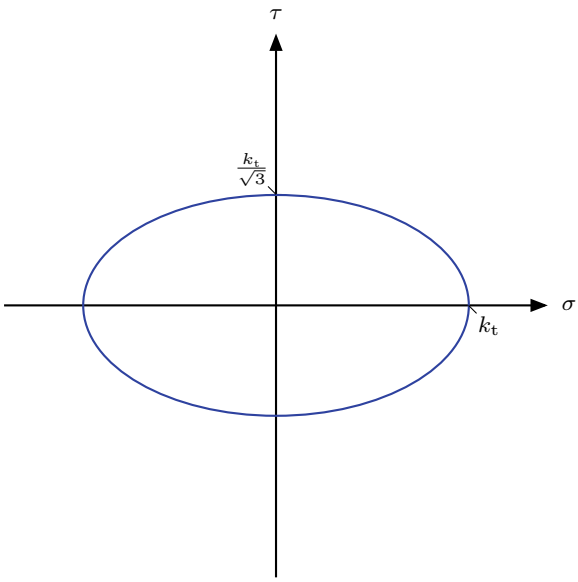

Fig. 4.10 Graphical representation of the yield condition according to von Mises in the σ-τ space

$$k_s = \frac{k_t}{\sqrt{3}}. \tag{4.53}$$

Based on this relation, it is possible to express the yield condition in terms of the shear yield stress, for example, as:

$$F(J_2') = \sqrt{J_2'} - k_s = 0. \tag{4.54}$$

Table 4.8 illustrates the fact that it is not the right approach to look on single stress components if one has to judge if the stress state is in the elastic or already in the plastic domain. Only the equivalent stress based on a yield condition can answer this question in the case of multiaxial stress states.

4.3.2 Tresca Yield Condition

The Tresca yield condition, also known as the maximum shear stress theory, postulates yielding as soon as the maximum shear stress reaches an experimental value. This yield condition is commonly applied for ductile metals. The expression is given for the principal stresses as

$$\max\left(\frac{1}{2}|\sigma_1 - \sigma_2|, \frac{1}{2}|\sigma_2 - \sigma_3|, \frac{1}{2}|\sigma_3 - \sigma_1|\right) = k_s, \tag{4.55}$$

Table 4.8 Equivalent von Mises stress for different stress states

Stress matrix σ_{ij}	Von Mises stress Eq. (4.43)	Domain ($k_t^{init} = 150$)
$\begin{bmatrix} 100 & 0 & 0 \\ 0 & 100 & 0 \\ 0 & 0 & 0 \end{bmatrix}$	100	Elastic
$\begin{bmatrix} 100 & 0 & 0 \\ 0 & -100 & 0 \\ 0 & 0 & 0 \end{bmatrix}$	173.2	Plastic
$\begin{bmatrix} 200 & 0 & 20 \\ 0 & 80 & 20 \\ 20 & 20 & 90 \end{bmatrix}$	125.3	Elastic
$\begin{bmatrix} 200 & 0 & 20 \\ 0 & 80 & 20 \\ 20 & 20 & 200 \end{bmatrix}$	129.3	Elastic
$\begin{bmatrix} 100 & 0 & 20 \\ 0 & 80 & 20 \\ 20 & 20 & -80 \end{bmatrix}$	177.8	Plastic

or

$$F(\sigma_i) = \max\left(\frac{1}{2}|\sigma_1 - \sigma_2|, \frac{1}{2}|\sigma_2 - \sigma_3|, \frac{1}{2}|\sigma_3 - \sigma_1|\right) - k_s = 0. \tag{4.56}$$

Expressed with the second and third invariant of the stress deviator, the following formulation is obtained:

$$F(J_2', J_3') = 4\left(J_2'\right)^3 - 27\left(J_3'\right)^2 - 36k_s^2\left(J_2'\right)^2 + 96k_s^4 J_2' - 64k_s^6 = 0. \tag{4.57}$$

The graphical representation in the principal stress space is given in Fig. 4.11, where a prism of six sides with its longitudinal axis equal to the hydrostatic axis is obtained. The view along the hydrostatic axis is shown in Fig. 4.12, where a hexagon can be seen. In addition, it can be concluded that the tensile and compressive yield stresses have the same magnitude.

The representation in the $\sqrt{3J_2'}$-J_1° space (see Fig. 4.13) shows that the yield condition is independent of the hydrostatic stress.

For a representation in the two-component principal σ_1-σ_2 space, the following six straight-line equations can be derived from Eq. (4.55) (see Fig. 4.14):

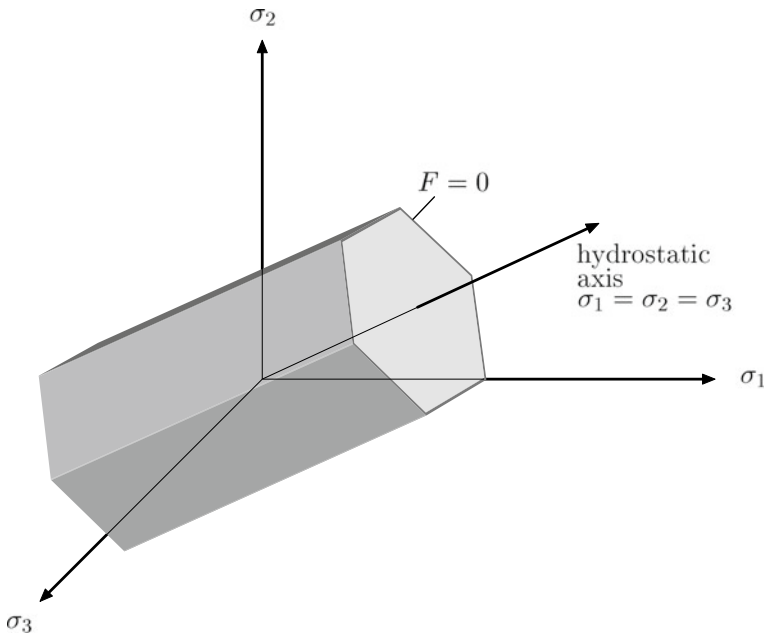

Fig. 4.11 Graphical representation of the yield condition according to Tresca in the principal stress space

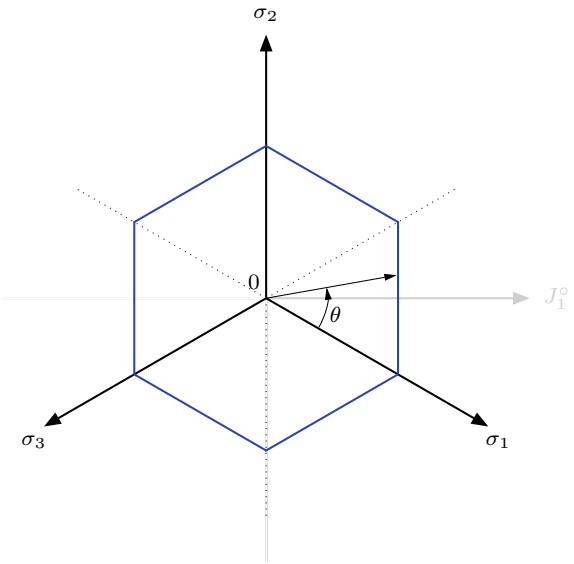

Fig. 4.12 Graphical representation of the yield condition according to Tresca in the octahedral plane

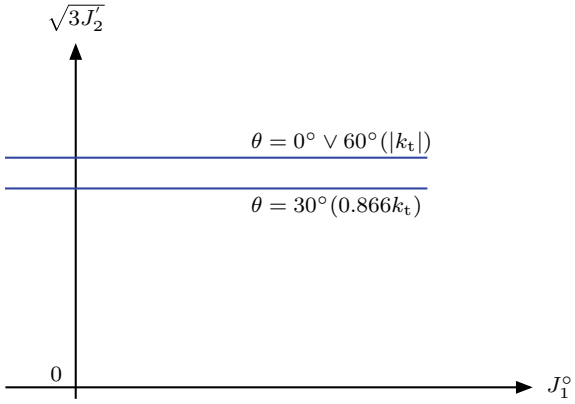

Fig. 4.13 Graphical representation of the yield condition according to Tresca in the $\sqrt{3J_2'}$-J_1° space

$$\begin{aligned}
\sigma_2^{(1)} &= \sigma_1 - 2k_s = \sigma_1 - k_t,\\
\sigma_2^{(2)} &= \sigma_1 + 2k_s = \sigma_1 + k_t,\\
\sigma_2^{(3)} &= 2k_s = k_t,\\
\sigma_2^{(4)} &= -2k_s = -k_t,\\
\sigma_1^{(5)} &= 2k_s = k_t,\\
\sigma_1^{(6)} &= -2k_s = -k_t.
\end{aligned} \tag{4.58}$$

The principal stresses[5] σ_1 and σ_2 result from Mohr's circle as

$$\sigma_1 = \frac{\sigma}{2} + \sqrt{\left(\frac{\sigma}{2}\right)^2 + \tau^2} \quad ; \quad \sigma_2 = \frac{\sigma}{2} - \sqrt{\left(\frac{\sigma}{2}\right)^2 + \tau^2}. \tag{4.59}$$

Substituting Eq. (4.59) into Eq. $(4.55)_1$ yields the yield condition in the $\sigma - \tau$ space as

$$F_{\sigma-\tau} = \left(\frac{\sigma}{2}\right)^2 + \tau^2 = k_s^2 \tag{4.60}$$

or (Fig. 4.15):

$$F_{\sigma-\tau} = \left(\frac{\sigma}{k_t}\right)^2 + \left(\frac{2\tau}{k_t}\right)^2 - 1. \tag{4.61}$$

[5] Mohr's circle gives $\sigma_1 > 0$ and $\sigma_3 < 0$ with $\sigma_2 = 0$.

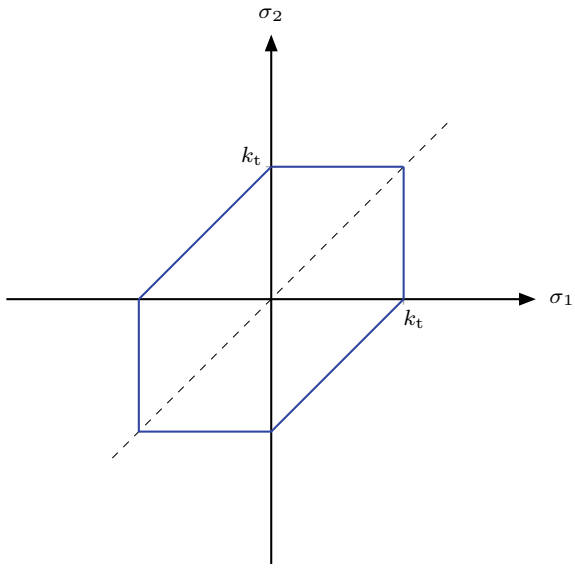

Fig. 4.14 Graphical representation of the yield condition according to Tresca in the σ_1–σ_2 space

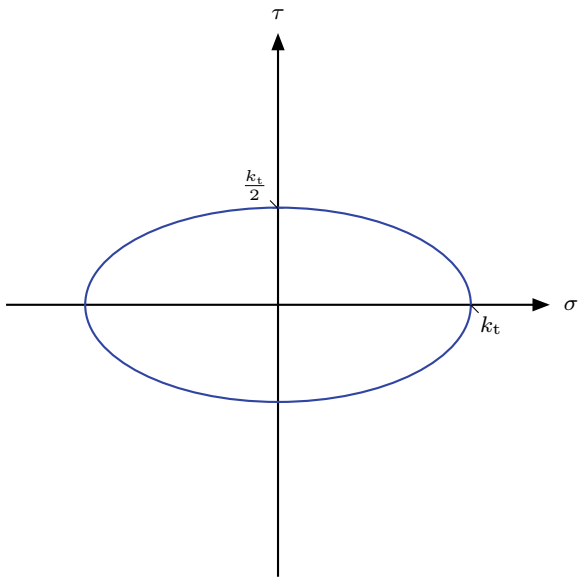

Fig. 4.15 Graphical representation of the yield condition according to Tresca in the σ–τ space

The last formulation allows to identify the relationship between the shear and tensile yield stress as:

$$k_\mathrm{s} = \frac{k_\mathrm{t}}{2}. \tag{4.62}$$

4.3.3 Drucker-Prager Yield Condition

The Drucker-Prager yield condition is an extension of the formulation according to von Mises [see Eq. (4.54)], which considers the influence of the weighted (factor α) hydrostatic stress (J_1^o):

$$F(J_1^\mathrm{o}, J_2') = \alpha J_1^\mathrm{o} + \sqrt{J_2'} - k_\mathrm{s}, \tag{4.63}$$

where the α and k_s are the material parameters. It should be noted here that the von Mises yield condition is included in Eq. (4.63) for $\alpha = 0$. This condition is usually applied as a failure condition for soils, rocks, and concrete.

The representation in the $\sqrt{J_2'}$-J_1° space (see Fig. 4.16) shows that the yield condition is linearly dependent on the hydrostatic stress. This behavior would represent in the principal stress space a right-circular cone.

The view along the hydrostatic axis is shown in Fig. 4.17 where it can be seen that, as in the case of von Mises, a circle is obtained. However, the radius is now a function of the hydrostatic stress, i.e., $r = \sqrt{2}(k_\mathrm{s} - \alpha J_1^\circ)$. This radius reduces in the π-plane, meaning for $J_1^\circ = 0$ or $\sigma_\mathrm{m} = 0$, to $r = \sqrt{2}k_\mathrm{s}$, which is identical to the constant radius of the von Mises yield condition, see Fig. 4.8 and relation (4.53).

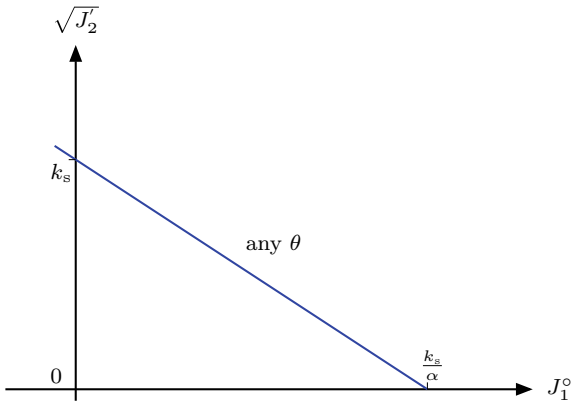

Fig. 4.16 Graphical representation of the yield condition according to Drucker-Prager in the $\sqrt{J_2'}$-J_1° space

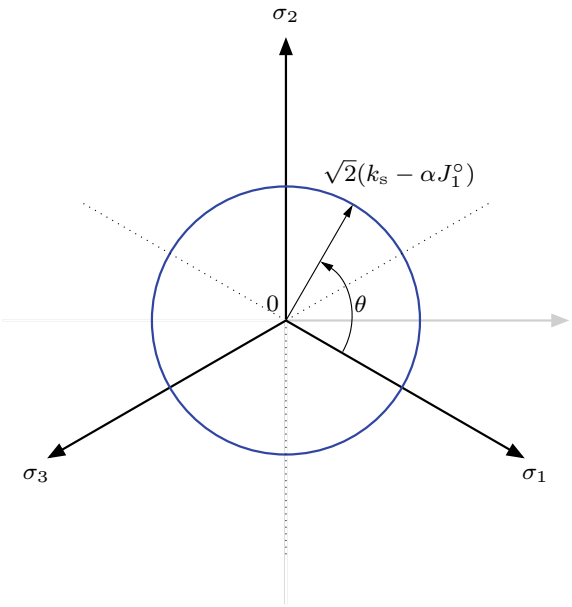

Fig. 4.17 Graphical representation of the yield condition according to Drucker-Prager in an octahedral plane ($\sigma_m = \text{const.}$)

Substituting the equations from Table 4.5 for the basic invariants into Eq. (4.63), the representation in the two-component principal σ_1–σ_2 space is obtained as

$$F_{\sigma_1-\sigma_2} = \left(1 - 3\alpha^2\right)\left(\sigma_1^2 + \sigma_2^2\right) - \left(1 + 6\alpha^2\right)\sigma_1\sigma_2 + 6\alpha k_s\left(\sigma_1 + \sigma_2\right) - 3k_s^2, \quad (4.64)$$

or after some transformations the equation of a shifted and rotated ellipse in the $\sigma_1 - \sigma_2$ space is obtaind as (see Fig. 4.18):

$$F_{\sigma_1-\sigma_2} = \left(\frac{x + \frac{6\sqrt{2}k_s\alpha}{1-12\alpha^2}}{\frac{\sqrt{6}k_s}{1-12\alpha^2}}\right)^2 + \left(\frac{y}{\frac{\sqrt{2}k_s}{\sqrt{1-12\alpha^2}}}\right)^2 - 1, \quad (4.65)$$

where

$$x = \frac{1}{\sqrt{2}}\left(\sigma_1 + \sigma_2\right), \quad y = \frac{1}{\sqrt{2}}\left(\sigma_2 - \sigma_1\right). \quad (4.66)$$

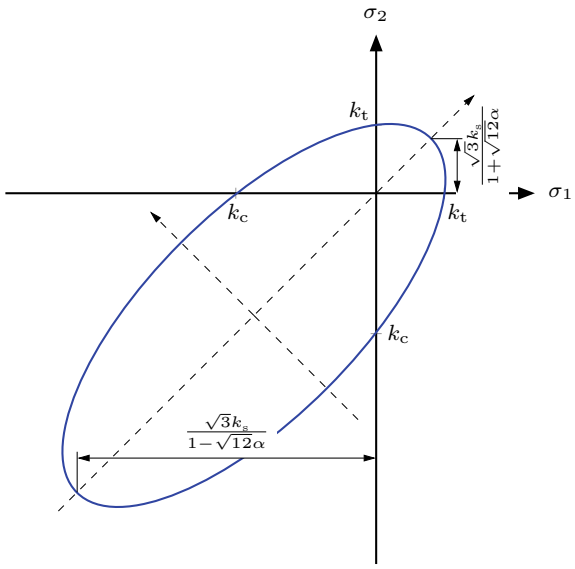

Fig. 4.18 Graphical representation of the yield condition according to Drucker-Prager in the σ_1-σ_2 space

The transformation of Eq. (4.64) into Eq. (4.65) can be obtained in the following way:

$$
\begin{aligned}
&\frac{1}{3}\left(\sigma_1^2+\sigma_2^2-\sigma_1\sigma_2\right)=k_s^2-2k_s\alpha\left(\sigma_1+\sigma_2\right)+\alpha^2\left(\sigma_1+\sigma_2\right)^2 \mid \times 12,\\
&4\left(\sigma_1^2+\sigma_2^2-\sigma_1\sigma_2\right)=12k_s^2-24k_s\alpha\left(\sigma_1+12\sigma_2\right)+12\alpha^2\left(\sigma_1+\sigma_2\right)^2,\\
&\sigma_1^2+2\sigma_1\sigma_2+\sigma_2^2+3\left(\sigma_1^2-2\sigma_1\sigma_2+\sigma_2^2\right)=12k_s^2-24k_s\alpha\left(\sigma_1+12\sigma_2\right)+\\
&\qquad+12\alpha^2\left(\sigma_1+\sigma_2\right)^2,\\
&\left(\sigma_1+\sigma_2\right)^2+3\left(\sigma_1-\sigma_2\right)^2=12k_s^2-24k_s\alpha\left(\sigma_1+12\sigma_2\right)+12\alpha^2\left(\sigma_1+\sigma_2\right)^2,\\
&\left(\sigma_1+\sigma_2\right)^2+3\left(\sigma_1-\sigma_2\right)^2+24k_s\alpha\left(\sigma_1+12\sigma_2\right)-12\alpha^2\left(\sigma_1+\sigma_2\right)^2=\\
&\quad=\left(\frac{12k_s^2}{1-12\alpha^2}-\frac{12\alpha^2k_s^2}{1-12\alpha^2}\right),\\
&3\left(1-12\alpha^2\right)\left(\sigma_1-\sigma_2\right)^2+\left(1-12\alpha^2\right)^2\left(\sigma_1+\sigma_2\right)^2+\\
&\qquad+2\times12k_s\alpha\left(1-12\alpha^2\right)\left(\sigma_1+\sigma_2\right)+12^2\alpha^2k_s^2=12k_s^2,\\
&3\left(1-12\alpha^2\right)\left(\sigma_1-\sigma_2\right)^2+\left(\left(1-12\alpha^2\right)\left(\sigma_1+\sigma_2\right)+12k_s\alpha\right)^2=12k_s^2,\\
&\frac{\left(1-12\alpha^2\right)\left(\sigma_1-\sigma_2\right)^2}{4k_s^2}+\frac{\left(\left(1-12\alpha^2\right)\left(\sigma_1+\sigma_2\right)+12k_s\alpha\right)^2}{12k_s^2}=1.
\end{aligned}
\tag{4.67}
$$

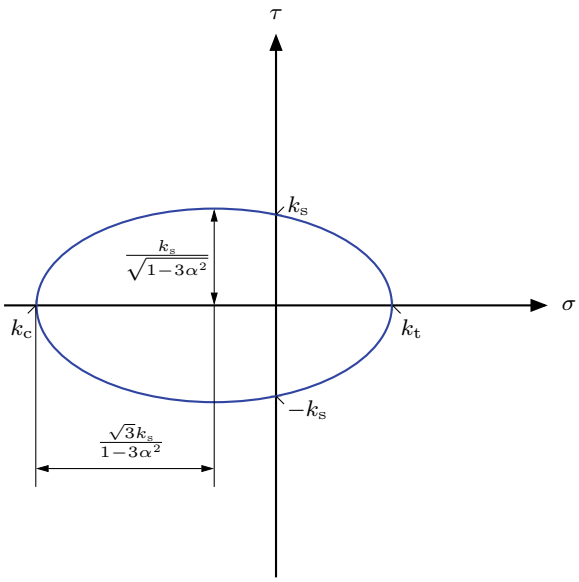

Fig. 4.19 Graphical representation of the yield condition according to Drucker-Prager in the σ-τ space

The same procedure yields under consideration of $k_s^2 = \frac{k_s^2}{1-3\alpha^2} - \frac{3\alpha^2 k_s^2}{1-3\alpha^2}$ also to a shifted ellipse in the $\sigma - \tau$ space (see Fig. 4.19):

$$\left(\frac{\sigma + \frac{3k_s\alpha}{1-3\alpha^2}}{\frac{\sqrt{3}k_s}{1-3\alpha^2}}\right)^2 + \left(\frac{\tau}{\frac{k_s}{\sqrt{1-3\alpha^2}}}\right)^2 - 1. \tag{4.68}$$

Setting $\tau \to 0$ in the last relation allows to extract the relation between the tensile/compressive yield stress and the shear limit ($\sigma \to k_t \wedge \sigma \to k_c$) as:

$$k_t = \frac{\sqrt{3}}{1+\sqrt{3}\alpha}k_s, \quad k_c = \frac{\sqrt{3}}{1-\sqrt{3}\alpha}k_s. \tag{4.69}$$

Finally, it should be noted here that also the formulation

$$F(J_1^o, J_2') = \alpha J_1^o + \sqrt{J_2'} - \frac{\bar{\sigma}}{\sqrt{3}}, \tag{4.70}$$

where

$$\bar{\sigma} = (1 + \alpha\sqrt{3})k_t \tag{4.71}$$

and the alternative term linear Mohr-Coulomb can be found in literature.

4.4 Flow Rule

The flow rule, which allows the evaluation of the plastic strain increments, in its general form is given by

$$\mathrm{d}\boldsymbol{\varepsilon}^{\mathrm{pl}} = \mathrm{d}\lambda\, \boldsymbol{r}(\boldsymbol{\sigma}, \boldsymbol{q}), \tag{4.72}$$

where $\mathrm{d}\lambda$ is a scalar called the plastic multiplier or consistency parameter and function $\boldsymbol{r}(\boldsymbol{\sigma}, \boldsymbol{q}) : (\mathrm{IR}^6 \times \mathrm{IR}^{\dim(q)} \rightarrow \mathrm{IR}^6)$ is the plastic flow direction. The plastic flow direction is often stated in terms of a plastic potential function Q, and the plastic strain increments are given by $\mathrm{d}\boldsymbol{\varepsilon}^{\mathrm{pl}} = \mathrm{d}\lambda \frac{\partial Q}{\partial \boldsymbol{\sigma}}$. The flow is said to be associated if $Q = F$, otherwise non-associated.

The evolution equation for the internal variables $\boldsymbol{q}$ can be specified in its general form as

$$\mathrm{d}\boldsymbol{q} = \mathrm{d}\lambda\, \boldsymbol{h}(\boldsymbol{\sigma}, \boldsymbol{q}), \tag{4.73}$$

where the function $\boldsymbol{h} : (\mathrm{IR}^6 \times \mathrm{IR}^7 \rightarrow \mathrm{IR}^7)$ describes the evolution of the hardening parameters.

4.5 Hardening Rule

The hardening rule allows the consideration of the influence of material hardening on the yield condition and the flow rule.

4.5.1 Isotropic Hardening

In the case of isotropic hardening, the yield stress is expressed as being dependent on an inner variable κ:

$$k = k(\kappa). \tag{4.74}$$

This results in the effect that the size of the yield surface is scaled but the origin remains unchanged. If the equivalent plastic strain[6] is used for the hardening variable ($\kappa = \varepsilon^{\mathrm{pl}}_{\mathrm{eff}}$), then one talks about strain hardening.

Another possibility is to describe the hardening being dependent on the specific[7] plastic work ($\kappa = w^{\mathrm{pl}} = \int \boldsymbol{\sigma}\, \mathrm{d}\boldsymbol{\varepsilon}^{\mathrm{pl}}$). Then one talks about work hardening.

---

[6] The effective plastic strain is in the general three-dimensional case the function $\varepsilon^{\mathrm{pl}}_{\mathrm{eff}} : (\mathrm{IR}^6 \rightarrow \mathrm{IR}_+)$ with $\varepsilon^{\mathrm{pl}}_{\mathrm{eff}} = \sqrt{\frac{2}{3}\boldsymbol{\varepsilon}^{\mathrm{pl}}\boldsymbol{\varepsilon}^{\mathrm{pl}}}$.

[7] This is the volume-specific definition, meaning $\left[w^{\mathrm{pl}}\right] = \frac{\mathrm{N}}{\mathrm{m}^2}\frac{\mathrm{m}}{\mathrm{m}} = \frac{\mathrm{kg\,m}}{\mathrm{s}^2\mathrm{m}^2}\frac{\mathrm{m}}{\mathrm{m}} = \frac{\mathrm{kg\,m}^2}{\mathrm{s}^2\mathrm{m}^3} = \frac{\mathrm{J}}{\mathrm{m}^3}$.

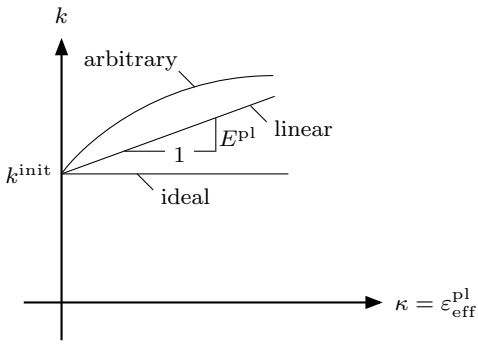

Fig. 4.20 Flow curve for different isotropic hardening laws. The abscissa is drawn for the case of strain hardening

Figure 4.20 shows different modeling approaches for the flow curve, meaning the graphical illustration of the yield stress being dependent on the inner variable for different hardening approaches.

4.5.2 Kinematic Hardening

In the case of pure kinematic hardening, the yield condition is expressed as being dependent on a set of inner variables:

$$F(\boldsymbol{\sigma}, \boldsymbol{\alpha}) = f(\boldsymbol{\sigma} - \boldsymbol{\alpha}) - k = 0, \tag{4.75}$$

where the material parameter k is constant and the kinematic hardening parameters $\boldsymbol{\alpha}$ are dependent on inner variables. These hardening parameters represent the center of the yield surface and result in the effect that the surface translates as a rigid body in the stress space.

References

Altenbach H, Altenbach J, Zolochevsky A (1995) Erweiterte Deformationsmodelle und Versagenskriterien der Werkstoffmechanik. Deutscher Verlag für Grundstoffindustrie, Stuttgart
Altenbach H (2012) Kontinuumsmechanik: Einführung in die materialunabhängigen und materialabhängigen Gleichungen. Springer, Berlin
Altenbach H, Öchsner A (eds) (2020) Encyclopedia of continuum mechanics. Springer, Berlin
Asaro RJ, Lubarda VA (2006) Mechanics of solids and materials. Cambridge University Press, Cambridge
Backhaus G (1983) Deformationsgesetze. Akademie-Verlag, Berlin
Betten J (1987) Tensorrechnung für Ingenieure. Teubner Verlag, Stuttgart
Betten J (2001) Kontinuumsmechanik. Springer, Berlin

Chen WF, Han DJ (1988) Plasticity for structural engineers. Springer, New York
Chen WF, Zhang H (1991) Structural plasticity: theory, problems, and CAE software. Springer, New York
Gurson AL (1977) Continuum theory of ductile rupture by void nucleation and growth: part I—yield criteria and flow rules for ductile media. J Eng Mater-T ASME 99:2–15
Itskov M (2009) Tensor algebra and tensor analysis for engineers: with applications to continuum mechanics. Springer, Berlin
Lurie AI, Belyaev A (2005) Theory of Elasticity. Springer, Berlin
Moore TA (2013) A general relativity workbook. University Science Books, Mill Valley
Nash WA (1998) Schaum's outline of theory and problems of strength of material. McGraw-Hill, New York
Nayak GC, Zienkiewicz OC (1972) Convenient form of stress invariants for plasticity. J Struct Div-ASCE 98:1949–954
Öchsner A (2003) Experimentelle und numerische Untersuchung des elastoplastischen Verhaltens zellularer Modellwerkstoffe. VDI-Verlag, Düsseldorf
Öchsner A (2016) Continuum damage and fracture mechanics. Springer, Singapore
Suzuki H, Ninomiya T, Sumino K, Takeuchi (1985) Dislocation in solids: proceedings of the IX Yamada. VNU Science Press, Utrecht